Neuropilin-2 acts a critical determinant for epithelial-to-mesenchymal transition progression and aggressive behaviors of human head and neck cancervia the RSK1/Sox2/Zeb1 signaling pathway

Min-Hye Ahn
Seoul National University School of Dentistry
Ji-Hoon Kim
Seoul National University School of Dentistry
Su-Jung Choi
Seoul National University School of Dentistry
Hyun-Ji Kim
Seoul National University School of Dentistry
Dong-Guk Park
Seoul National University School of Dentistry
Kyu-Young Oh
Dankook University College of Dentistry
Hye-Jung Yoon
Seoul National University School of Dentistry
Seong-Doo Hong
Seoul National University School of Dentistry
Jae-Il Lee
Seoul National University School of Dentistry
Ji-Ae Shin
Seoul National University School of Dentistry
Sung-Dae Cho (efiwdsc@snu.ac.kr)
Seoul National University https://orcid.org/0000-0001-8670-9579

Research

Keywords: Head and neck cancer, Neuropilin-2, Metastasis, Epithelial-to-mesenchymal transition, Codium fragile

Posted Date: March 24th, 2023

DOI: https://doi.org/10.21203/rs.3.rs-2698249/v1

Abstract

Background

Neuropilin-2 (NRP2) is a multifunctional single-pass transmembrane receptor that binds to two disparate ligands, namely, vascular endothelial growth factors (VEGFs) and semaphorins (SEMAs). It is reportedly involved in neuronal and vascular development. In this study, we uncovered the exact functional role of NRP2 and its molecular mechanism during aggressive behaviors and lymph node (LN) metastasis in human head and neck cancer (HNC) and identified algal methanol extract as a potential novel NRP2 inhibitor.

Methods In silico

analyses and immunohistochemistry were used to investigate the relationship between NRP2 expression and the prognosis of HNC patients. The functional role of NRP2 on the proliferation, migration, invasion, and cancer stem cell (CSC) properties of HNC cells was examined by MTS, soft agar, clonogenic, transwell migration and invasion assays, and sphere formation assays. Signaling explorer antibody array, western blot, and qPCR were performed toward the investigation of a molecular mechanism that is related to NRP2.

Results

NRP2 was highly expressed in HNC and positively correlated with LN metastasis and advanced tumor stage and size in patients. Using loss- or gain-of-function approaches, we found that NRP2 promoted the proliferative, migratory, and invasive capacities of human HNC cells. Furthermore, NRP2 regulated Sox2 expression to exhibit aggressiveness and CSC properties of human HNC cells. We demonstrated that p90 ribosomal S6 kinase 1 (RSK1) elevates the aggressiveness and CSC properties of human HNC cells, possibly by mediating NRP2 and Sox2. Zeb1 was necessary for executing the NRP2/RSK1/Sox2 signaling pathway during the induction of epithelial-to-mesenchymal transition (EMT) and aggressive behaviors of human HNC cells. Moreover, the methanol extract of *Codium fragile* (MECF) repressed NRP2 expression, inhibiting the RSK1/Sox2/Zeb1 axis, which contributed to the reduction of aggressive behaviors of human HNC cells.

Conclusions

These findings suggest that NRP2 is a critical determinant in provoking EMT and aggressive behaviors in human HNC through the RSK1/Sox2/Zeb1 axis, and MECF may have the potential to be a novel NRP2 inhibitor for treating metastasis in HNC patients.

Background

Initially, neuropilins (NRPs) were described as cell surface glycoproteins that act as co-receptors for semaphorins (SEMAs) and vascular endothelial growth factors (VEGFs) ligands in different extracellular domains. They are implicated in axon guidance during neural development and angiogenesis [1]. NRP2 is highly expressed in a variety of cancer cells and is involved in tumorigenesis, aggressiveness, and is characterized by its low sensitivity to chemotherapeutic drugs [2, 3]. Furthermore, NRP2 expression in breast cancer *in vivo* is responsible for tumor initiation, extravasation, or metastasis [4, 5]. In addition, silencing NRP2 in tumor-associated macrophages enables cytotoxic CD8 + T lymphocytes and natural killer cells to infiltrate tumors, resulting in an anti-tumor immune response by inhibiting immunosuppression [6]. Thus, NRP2 seems to be a valuable therapeutic target for cancer therapy, and targeting NRP2, which underpins cancer cell aggressiveness, should be exploited for treating metastasis in patients.

Marine algae have been extensively utilized in nutraceutical and pharmaceutical industries because of the beneficial effects of their abundant bioactive compounds [7]. *Codium fragile* (*C. fragile*), a species belonging to the genus *Codium*, is a green alga primarily distributed in East Asia, Oceania, and North Europe [8]. Furthermore, *C. fragile* extracts have anti-obesity effects, as evidenced by improved intestinal metabolism via the regulation of gut microbiota composition [9]. *C. fragile* extracts have also been demonstrated to be potential anti-osteoarthritic agents by inhibiting nuclear translocation of NF-κB in IL-1β-induced rat primary cultured chondrocytes as well as by reducing the phosphorylation of ERK1/2 and JNK [10]. In artificial skin models and clinical studies, extracellular vesicles of *C. fragile* suppressed melanin synthesis, indicating their potential as skin brightness agents [11]. Furthermore, previous studies have demonstrated that *C. fragile* extracts and their isolated derivatives have anti-cancer activities. For example, the methanol extract of *C. fragile* suppresses the invasion property of human breast cancer cells by repressing the NF-κB/MMP9 axis [12]. Polysaccharides isolated from *C. fragile* have been shown to enhance the effectiveness of cancer therapy by inducing an immune response through the activation of natural killer cells and dendritic cells [13, 14]. However, despite the fact that *C. fragile* appears to be valuable as a cancer therapeutic for future applications, EMT progression and aggressive behaviors of *C. fragile* during cancer metastatic cascades have not been widely investigated.

In this study, we investigate the functional significance of NRP2 as a critical determinant of EMT and aggressive behavior in human HNC by triggering the RSK1/Sox2/Zeb1 axis. Furthermore, we also provide a foundation for demonstrating the possibility of using MECF as a novel NRP2 inhibitor in the treatment of metastatic HNC.

Results

High expression of NRP2 is positively associated with worse prognosis in human HNC

To identify the value of NRP2 as a potential biomarker involved in tumorigenesis, we first analyzed the expression levels of NRP2 in normal tissues and nine kinds of human cancer tissues from the UALCAN database. The expression levels of NRP2 were highly expressed in all cancer types, including head and neck squamous cell carcinoma, compared to normal tissues (Fig. 1a). Correlation analysis, based on the cBioPortal dataset, demonstrated that the copy number of NRP2 is correlated with its mRNA levels in HNC samples (Fig. 1b). We further analyzed the mRNA levels of NRP2 based on GEO or TCGA datasets, which demonstrated that NRP2 mRNA levels in HNC tissues were significantly higher than those in normal or margin tissues (Figs. 1c-1e and S1). Further analysis of the CPTAC database comparing normal and tumor tissues showed that the NRP2 protein was present at higher levels in HNC tissues than in normal tissues (Fig. 1f). In contrast, there were no differences in NRP1 mRNA levels between the normal and HNC tissues (Figs. S2a-S2d). These results indicate that NRP2 can be a potential diagnostic marker for patients with HNC. To validate the results, using *in silico* analyses, we performed IHC staining of tissue samples from 53 OSCC cases, then classified them into low and high NRP2 expression groups. The intensity of NRP2 staining was remarkably higher in OSCC tissues than in the adjacent non-tumor epithelium (Fig. S3). Through multivariable analysis of NRP2 expression and clinicopathological characteristics, we observed that NRP2 expression positively associated with tumor stage, advanced tumor size, and lymph node (LN) metastasis in patients with OSCC (Table 1 and Fig. 1g). Notably, NRP2 was found to be more intense in cases with LN metastasis than in those without a history of LN metastasis (Fig. 1h). Furthermore, the expression pattern image between NRP2 expression and the final scores indicated that high expression of NRP2 significantly associated with LN metastasis in patients with OSCC (Figs. 1i and 1j). Consistently, NRP2 mRNA levels in LN-positive HNC samples, extracted from the GEO dataset, were statistically significant, compared with those in the LN-negative HNC samples (Fig. 1k). KM plotter analysis revealed that HNC patients with high NRP2 expression had a significantly adverse outcome (Fig. 1l). These results suggest that high NRP2 expression in HNC is positively associated with worse prognosis.

Table 1
Association between NRP2 expression and clinicopathological factors of OSCC patients

Variable	No. of cases (N = 53)	NRP2		*P value*	Risk ratio	95% CI
		Low (N = 30)	High (N = 23)			
Age						
< 58	27	15	12	0.875	1.05	0.57–1.94
≥ 58	26	15	11		0.95	0.51–1.76
Gender						
Male	36	21	15	0.712	0.89	0.47–1.67
Female	17	9	8		1.13	0.60–2.13
Differentiation status						
Well	36	22	14	0.335	0.73	0.40–1.35
Moderately	17	8	9		1.36	0.74–2.50
Tumor size						
T1 + T2	32	24	8	**0.001***	0.35	0.18–0.68
T3 + T4	21	6	15		2.86	1.48–5.52
LN metastasis						
Negative	32	23	9	**0.006***	0.42	0.22–0.79
Positive	21	7	14		2.37	1.26–4.46
Distant metastasis						
Negative	52	29	23	1.000	1.77	0.16–19.93
Positive	1	1	0		0.56	0.05–6.34
Stage						
I + II	24	20	4	**< 0.001***	0.25	0.10–0.65
III + IV	29	10	19		3.93	1.55–9.99
Recurrence						
No	41	21	20	0.144	1.95	0.70–5.46

Variable	No. of cases (N = 53)	NRP2		*P value*	Risk ratio	95% CI
		Low (N = 30)	High (N = 23)			
Yes	12	9	3		0.51	0.18–1.43

Nrp2 Promotes Proliferation, Motility, And Invasiveness Of Human Hnc Cells

We used NRP2-silencing HNC cells to obtain *in vitro* evidence supporting the relationship between NRP2 expression and aggressive behaviors in human HNC. First, we examined the expression levels of NRP2 in nine HNC cell lines and in a normal oral keratinocyte (HOK) cell line. The results demonstrated that NRP2 was remarkably overexpressed in all HNC cell lines compared to that in HOK cells (Fig. S4). We chose HSC-4, FaDu, and HN22 from among the HNC cell lines with high NRP2 expression levels to create NRP2-silencing cells. Real-time PCR and immunoblotting analyses verified that both mRNA and protein levels of NRP2 were significantly downregulated in the established NRP2-silencing cells (Figs. 2a and 2b). To define the functional role of NRP2 in the progression and tumorigenic potential of HNC *in vitro*, we conducted MTS, soft agar, and clonogenic assays using three NRP2-silencing cells. According to the findings, NRP2-silencing cells' proliferation and colony-forming capacities were slower or smaller than those of the respective control group (Fig. 2c-2e). Interestingly, with respect to morphological features, NRP2-silencing cells exhibited an epithelial-like phenotype with a polygonal shape, compared with the control groups, representing a mesenchymal-like phenotype with a spindle shape (Fig. 2f). To examine the role of NRP2 in the aggressive behavior of human HNC *in vitro*, we evaluated the motility and invasive abilities of NRP2-silencing cells using transwell migration and invasion assays. As shown in Fig. 2g, a significant reduction in migratory or invasive cells crossing the membranes was observed in the NRP2-silencing groups, compared to that in the control groups. These results demonstrated that NRP2 is required for the proliferation, motility, and invasiveness of human HNC.

Nrp2 Regulates Sox2 Expression To Promote Aggressiveness And Csc Properties Of Human Hnc Cells

To identify the molecular mechanism by which NRP2 exhibits aggressive behavior in human HNC *in vitro*, we performed a signaling explorer antibody array, consisting of 1,358 antibodies. Among them, 32 proteins with a fold shift greater than 1.2 in NRP2-silencing cells were selected (Fig. 3a). A previous study reported that mRNA levels of CSC markers such as Sox2, BMI-1, and Oct4 were upregulated during NRP2 overexpression in breast cancer cells [4]. Indeed, in our hierarchical clustering analysis, we observed a reduction in Sox2 enrichment in the NRP2-silencing group compared to the control group. This result was verified by immunoblotting (Fig. 3b). Next, we analyzed the CPTAC dataset to evaluate the relationship between NRP2 and Sox2 proteins in HNC samples, and the results showed a positive correlation between

NRP2 and Sox2 proteins (Fig. 3c). To explore the biological function of Sox2 in human HNC *in vitro*, the endogenous levels of Sox2 in the two HNC cell lines were knocked down using siRNA. After confirming the reduced endogenous levels of Sox2 in both cell lines (Fig. 3d), we examined the effect of Sox2 knockdown on motility and invasiveness. As per the results, knocking down endogenous Sox2 in human HNC cells resulted in much weaker migratory or invasive capacities than those in the control group (Figs. 3e and 3f). To clarify the contribution of NRP2 expression to CSC stemness in human HNC cells, we performed a sphere-formation assay in NRP2-silencing cells. As shown in Fig. 3g, the sphere-forming abilities of NRP2-silencing cells were reduced compared to those of control cells. In addition, the expression levels of CSC markers, such as Nanog, were commonly reduced in the two NRP2-silencing cells compared with another CSC marker, Oct4 (Fig. S5a). These results demonstrated that Sox2 may be a critical factor in the NRP2 signaling pathway that is involved in the aggressiveness and CSC properties of HNC cells.

Rsk1 Mediates Between Nrp2 And Sox2 During Aggressive Behaviors Of Human Hnc Cells

To determine which protein kinase is an important determinant between NRP2 and Sox2 during the aggressive behaviors of human HNC cells, we examined the data from the signaling explorer antibody array. As shown in Fig. S6, five ribosomal protein kinases, RPS27 (MPS1), RPS6KA1 (RSK1), RPS6KA2 (RSK3), RPS6KA6 (RSK4), and RPS6KB1 (p70S6Kα), were chosen for validation. Of which, only RPS6KA1 (hereafter referred to as RSK1) exhibited a statistically significant decrease in NRP2-silencing cells compared to that in control cells (fold change = 0.56, $p = 0.020$). Furthermore, immunoblotting analysis verified that NRP2 silencing markedly reduced the expression levels of RSK1 and p-p90RSK (Fig. 4a). To clarify whether RSK1 mediates the relationship between NRP2 and Sox2, we evaluated the effect of the RSK inhibitor BI-D1870 on Sox2 expression. The results showed that BI-D1870 treatment suppressed the expression levels of both p-p90RSK and RSK1 in the two human HNC cell lines, which was accompanied by a significant reduction in Sox2 expression (Fig. 4b). We further examined whether RSK1 is necessary for the aggressive behavior of human HNC cells. After confirming the minimal effect of BI-D1870 on cell viability (Fig. 4c), we observed that BI-D1870 strongly inhibited the migratory and invasive capacities of human HNC cells (Figs. 4d and 4e). Furthermore, BI-D1870 treatment significantly reduced the ability of human HNC cells to form spheres when compared to control cells (Fig. 4f). Consistent with the results from NRP2-silencing cells, only Nanog was significantly decreased in BI-D1870-treated cells (Fig. S5b). These results demonstrate that RSK1 promotes the aggressiveness and CSC properties of human HNC cells, possibly by mediating the interaction between NRP2 and Sox2.

NRP2 is required for proliferation and aggressive behaviors of human HNC cells by activating the RSK1/Sox2 signaling pathway

To determine whether NRP2 is an important molecule for the RSK1/Sox2 signaling pathway, NRP2-overexpressing cells were established using the HSC-2 cell line, which expresses NRP2 at a low level.

Immunoblotting analysis showed that the expression levels of p-p90RSK, RSK1, and Sox2 in NRP2-overexpressing cells were significantly higher than those in the control cells (Fig. 5a). We next investigated the tumorigenic potential of NRP2 in human HNC cells using soft agar and clonogenic assays, which revealed that the colony-forming capacity of NRP2-overexpressing cells increased (Figs. 5b and 5c). Furthermore, NRP2 overexpression markedly increased the migratory and invasive abilities of HSC-2 cells (Figs. 5d and 5e). The sphere-forming ability of NRP2-overexpressing cells was greater than that of the control cells (Fig. 5f). Consistently, the protein levels of Nanog were higher in NRP2-overexpressing cells than in the control cells (Fig. S5c). These results indicate that NRP2 promotes proliferation and aggressive behavior of human HNC cells by activating the RSK1/Sox2 signaling pathway.

Zeb1 Is Involved In Emt Progression Of Human Hnc Cells During The Nrp2/rsk1/sox2 Signaling Pathway

Since NRP2-silencing cells exhibited an epithelial-like phenotype, we further investigated the relationship between the NRP2/RSK1/Sox2 signaling pathway and EMT-related proteins. Among the seven EMT-related proteins, including mesenchymal and epithelial markers, the expression of mesenchymal marker Zeb1 was lower in two NRP2-silencing cells than in control cells, whereas the expression of the epithelial marker E-cadherin was higher in NRP2-silencing cells (Fig. 6a). In addition, the expression levels of Zeb1 were effectively reduced in both siSox2-transfected and BI-D1870-treated cells (Figs. 6b and 6c). However, NRP2 overexpression had the opposite effect (Fig. 6d). These results provide evidence that Zeb1 may be a crucial determinant of the NRP2/RSK1/Sox2 signaling pathway for EMT progression in human HNC cells.

Mecf Inhibits The Aggressiveness Of Human Hnc Cells By Suppressing Nrp2/rsk1/sox2/zeb1 Signaling Pathway

To discover the novel NRP2 inhibitor that inhibits aggressive behaviors of human HNC cells, the HNC cells were treated with 20 kinds of algal methanol extracts at the same dose for 48 h. Even though the viability of cells treated with algal methanol extracts did not change, only extract No. 17 remarkably suppressed the expression of NRP2, compared with other extracts (Figs. S7a and S7b). We further verified that the No. 17 extract (hereafter called MECF) decreased the expression levels of NRP2 in the three human HNC cell lines (Fig. 7a). To evaluate whether MECF regulates the motility and invasiveness of human HNC cells, we performed Transwell migration and invasion assays. The results revealed that the migratory and invasive abilities of HSC-4 and HN22 cells following MECF treatment were lower than those of the respective control cells, whereas MECF treatment only decreased the invasive ability of FaDu cells without affecting their migratory capacity (Figs. 7b and 7c). Nonetheless, MECF did not exhibit any noticeable cytotoxicity in the three human HNC cell lines (Fig. 7d). To determine whether MECF treatment regulated the RSK1/Sox2/Zeb1 signaling pathway, we performed immunoblotting analysis. As shown in

Fig. 7e, the expression levels of p-p90RSK, RSK1, Sox2, and Zeb1 were significantly reduced in MECF-treated cells compared to the respective control cells. Furthermore, we found that MECF strongly inhibited the sphere-forming ability of human HNC cells (Fig. 7f). In addition, MECF repressed the expression of Nanog and Oct4 in both HNC cell lines (Fig. S5d). These results indicate that MECF can be a potential NRP2 inhibitor that reduces the aggressive behavior of human HNC cells, possibly by inhibiting the RSK1/Sox2/Zeb1 signaling pathway.

Discussion

NRP2 is highly expressed in different types of tumors and is implicated in tumor development, progression, lymphangiogenesis, and lymphatic metastasis [15, 16]. Thus, NRP2 may be a valuable therapeutic target for cancer treatment. In this study, we found that high NRP2 levels in patients with HNC positively correlated with poor prognosis. Furthermore, our results demonstrated that NRP2 is responsible for EMT progression and aggressive behavior of human HNC cells. Similar to the oncogenic role of NRP2 during tumorigenesis, NRP1 is often upregulated in various types of cancer and participates in cancer progression and angiogenesis [15, 17, 18]. Furthermore, high levels of NRP1 allow cancer cells to be resistant to targeted therapy [19, 20] and may also promote immunosuppressive effects through enhanced T-regulatory cell (Treg) tumor infiltration [21]. However, results of *in silico* analysis reveal that the mRNA levels of NRP1 in normal and HNC tissues showed no variation, in contrast to NRP2. These results demonstrate that NRP2, but not NRP1, is predominantly expressed in HNC and may be an important regulator of HNC development.

The p90 ribosomal S6 kinase (RSK) family proteins, designated RSK1-4, are a group of serine/threonine kinases that have a high degree of structural similarity (approximately 73–80%) [22]. Despite the high similarity, RSK1 and RSK2 function as oncoproteins, which are often overexpressed in a variety of cancer types, contrary to RSK3 and RSK4, which have tumor-suppressive functions [22]. However, additional evidence supporting RSK isoform function also occasionally shows an opposite effect on cancer invasion and metastasis [23]. Although RSK1 depletion failed to reduce the invasiveness of human HNC cell lines [24], we found that inhibition of RSK1 using an RSK inhibitor suppressed the motility and invasive capacities of human HNC cells. A previous study reported that the pan-RSK inhibitor LJI308 that contributes to eradicating the population of cancer stem cells (CSC) is enriched in triple-negative breast cancer by inhibiting the oncogenic transcription factor YB-1, resulting in the avoidance of tumor recurrence [25]. Another classical pan-RSK inhibitor, BI-D1870, reduces CSC characteristics and reinforces the sensitivity of esophageal cancer cells to radiotherapy [26]. In this study, we also found that the reduction in RSK1 induced by the RSK inhibitor was sufficient to diminish the sphere-forming capacity of human HNC cells, which seemed to be implicated in a decrease in Sox2 and Nanog, which are key indicators of CSC stemness. Thus, it is possible that RSK1 is necessary for the maintenance of aggressive traits in human HNC cells through the regulation of stemness marker proteins, such as Sox2. An earlier investigation revealed that ERK/MAPK plays a pivotal role in mediating the NRP2 signaling pathway, which contributes to promoting tumorigenesis and metastasis in oesophageal cancer [27]. It has been noted that RSK proteins are one of the downstream targets of the Ras/Raf/MEK/ERK signaling

cascade in several cancer types, including prostate cancer [28]. In this study, the expression levels of RSK1 and p-p90RSK were found to be lowered in NRP2-silencing cells, whereas NRP2-overexpressing cells showed the opposite effect. Thus, a possible explanation for these findings is that RSK1 may be essential for NRP2 signaling, in which ERK/MAPK participates. Nonetheless, our findings suggest that RSK1 could be a critical route that links Sox2 via NRP2 signaling in human HNC cells, although additional investigation is required to ascertain whether ERK/MAPK plays a role in mediating the relationship between NRP2 and RSK.

EMT (known as a complete EMT) is a dynamic and reversible cellular program in which cells lose the epithelial cell-like properties, such as polygonal shape and cell to cell adhesion, and acquire mesenchymal cell-like traits, such as spindle shape and front-back cell polarity [29, 30]. Although EMT is necessary for embryogenesis and tissue regeneration in normal tissues, it also encourages cancer cells to gradually acquire aggressive traits in the metastatic cascade [31]. During this process, major EMT-inducing transcription factors (EMT-TFs), including Zeb1, Zeb2, Twist, Snail, and Slug, contribute to the repression of epithelial genes (*e.g.*, E-cadherin and ZO-1) and/or the induction of mesenchymal genes (*e.g.*, Fibronectin and Vimentin) [32]. In this study, we found that NRP2 silencing reduced the expression levels of Zeb1, a mesenchymal marker protein, in two HNC cell lines, which appeared to be mediated by the inhibition of the RSK1/Sox2 axis. Zeb1, a representative EMT-TF, acts as a transcriptional repressor of E-cadherin by interacting with BRG1 [33]. Thus, we speculated that the reduced expression of Zeb1 in NRP2-silencing cells would be capable of inducing the activation of E-cadherin expression. Unexpectedly, E-cadherin expression did not depend on the NRP2/RSK1/Sox2 axis (data not shown), even though its expression was significantly increased in NRP2-silencing cells. A previous study reported that the maintenance of E-cadherin is not necessary for the progression of c-erbB2-induced EMT [34]. Considering this, our results suggest that the maintenance of E-cadherin is not essential for suppressing EMT progression and aggressive behavior of human HNC cells through the NRP2/RSK1/Sox2/Zeb1 signaling pathway. NRP2 silencing was not responsible for inducing another epithelial marker or repressing other mesenchymal markers in either cell line. Cancer cells simultaneously express epithelial and mesenchymal characteristics without undergoing complete cellular changes during EMT progression, which is defined as partial EMT [35]. A recent study demonstrated that partial EMT, rather than complete EMT, contributes to metastatic tumor progression [36]. Therefore, our findings suggest that NRP2 acts as a critical regulator of EMT development in human HNC cells by modulating Zeb1 without the need to maintain E-cadherin.

Interestingly, in this study, we observed that MECF inhibited the invasive ability of FaDu cells without affecting their migratory capacity, in contrast to other cell lines. Earlier studies have reported that cell migration is defined as simply moving from one area to another [37], whereas cell invasion is the critical motile ability needed to infiltrate surrounding tissues by destroying the extracellular matrix [38]. Hence, cancer invasion is regarded as the initial stage of the metastatic cascade [39]. Evidence from a recent study found that celiensisin A derivative only suppressed the invasive characteristics of human bladder cancer cells by lowering Sox2 expression without showing a significant change in migration ability [40]. Based on these findings, we cannot exclude the possibility that MECF is more effective in suppressing the

invasion ability of human HNC cells than diminishing their migration capacity, even though the phenomenon seems to be cell context-dependent. Nonetheless, we found that MECF strongly suppressed the sphere-forming ability of HNC cells, including FaDu cells, which appeared to be attributed to a reduction in the NRP2/RSK1/Sox2/Zeb1 signaling pathway. Therefore, we suggest that MECF can be a potential NRP2 inhibitor that could reduce the aggressive behavior of human HNC cells.

Conclusion

In conclusion, our findings uncover the previously unknown signaling pathway of NRP2, which induces EMT and aggressive behavior in human HNC through the RSK1/Sox2/Zeb1 axis. We also identified MECF as a novel NRP2 inhibitor for treating metastasis in patients with HNC. Thus, our findings provide mechanistic insights into the oncogenic role of NRP2 as a potential therapeutic target for HNC metastasis and inspire the development of anticancer drugs derived from natural sources that target NRP2 in patients with metastatic HNC.

Methods

Clinical samples

From 2006 to 2007, paraffin-embedded OSCC samples were collected from patients diagnosed and surgically treated at the Department of Oral and Maxillofacial Surgery of the Seoul National University Dental Hospital (Seoul, Republic of Korea). Tumor classification for the TNM system was established according to the American Joint Committee on Cancer Manual. Tumor grades were based on the World Health Organization's classification of tumors. Clinicopathological factors, including age, sex, TNM classification, tumor stage, and recurrence, were collected from medical records. The characteristics of the 53 patients are presented in Table S2. All procedures were performed after obtaining approval from the Institutional Review Board of the Seoul National University Dental Hospital (IRB number: ERI20021).

Assessment Of Ihc Staining

Tissue sections were evaluated semi-quantitatively and independently reviewed by two pathologists without clinicopathological knowledge of the patient outcomes. If there was a slight disagreement between the two observers, they reappraised the consensus review. The definition of tumor proportion score (TPS) was classified as follows: 0, 0%; 1, 1–4%; 2, 5–49%; and 3, 50–100%. The staining intensity was scored as follows: 0, negative; 1, weak (light brown); and 2, strong (brown).

Preparation Of Algae Extracts And Pharmacological Reagent

C. fragile was collected from Sinji-do (Wando-gun, Republic of Korea) in December 2015. The MECF samples (unique identifier: TC15427) were kindly provided by the Chosun University (Gwangju, Republic

of Korea). All the algal methanol extracts used in this study are listed in Table S1. The RSK inhibitor, BI-D1870, was obtained from Abcam (Cambridge, MA, USA). All algal methanol extracts and BI-D1870 were dissolved in dimethyl sulfoxide (DMSO), aliquoted, and stored at − 20°C until use in the experiments. The final concentration of DMSO for each cell line did not exceed 0.1%.

Plasmid Construction

To construct a short hairpin RNA (shRNA) against human *NRP2*, a pLKO.1 puro vector was cloned with NRP2 shRNA oligonucleotides, as listed in Table S3. Two complementary oligonucleotides containing the target sequence were annealed and inserted into the pLKO.1 puro vector between the *Age* and *Eco*R sites according to Addgene's protocol. A scrambled shRNA without homology to other genes was used as a control vector. To construct the *NRP2* overexpressing vector, the open reading frame of human *NRP2* was synthesized by Bioneer (Daejeon, Republic of Korea) and cloned into the multi-cloning site of a pBabe puro IRES-EGFP vector. Viral vector information is listed in Table S4.

Virus Infection And Establishment Of Stable Cell Lines

For lentiviral packaging using the NRP2 silencing system, HEK293T cells were transfected with scramble shRNA or shNRP2, together with the pCMV-dR8.2 dvpr packaging vector and the pCMV-VSV-G envelope vector. For retroviral packaging using the NRP2 overexpression system, HEK293T cells were transfected with empty pBabe puro IRES-EGFP or pBabe-NRP2 overexpression vectors along with the pCL-10A1 packaging plasmid. All transfection procedures were carried out using Lipofectamine 2000 according to the manufacturer's instructions. After transfection for 48 h, the viral supernatants were collected and filtered through a 0.45-μm syringe filter. Purified viral supernatants were added to target cells with 6 μg/mL polybrene. The transduced cells were selected and maintained in complete medium containing puromycin. The vectors and reagents used in this study are presented in Table S4.

Small Interfering Rna (Sirna) Transfection

AccuTarget™ negative control siRNA (siControl) and a predesigned siRNA targeting human *Sox2* (siSox2) were purchased from Bioneer (Seongnam, Republic of Korea). Cells were transfected with either 40 nM siControl or siSox2 for specific time points (48 h for HSC-4 and 24 h for FaDu) using Lipofectamine 2000, following the manufacturer's instructions. The siRNAs targeting the human *Sox2* sequence are shown in Table S3.

Sphere Formation Assay

Cells were suspended in a serum-free medium containing 25 ng/mL of human epidermal growth factor (EGF), human basic fibroblast growth factor (bFGF), 0.01 X N-2 and B-27 supplements, and 1% P/S. The

cells (5×10^3 to 1×10^4 cells/well) were maintained in ultra-low attachment 6-well plates (Corning, Lowell, MA, USA) for 7 to 10 days. To calculate the sphere-forming efficiency, spheres larger than 50 μm in diameter were randomly captured using an inverted light microscope (Nikon, Tokyo, Japan) and then counted using ImageJ software (National Institutes of Health, Bethesda, MD, USA).

Signaling Explorer Antibody Array

HSC-4 cells stably expressing scramble shRNA or shNRP2 were prepared for the Signaling Explorer AB Array (Fullmoon Biosystems, Sunnyvale, CA, USA) consisting of 1,358 antibodies, and then analyzed using ebiogen (Seoul, Republic of Korea). Differentially expressed genes (DEGs) with a fold shift greater than 1.2 were identified using the Excel Based Differentially Expressed Gene Analysis (ExDEGA) v.2.5.0. The detailed procedures are illustrated in the Supplementary Materials and Methods.

Statistical analysis

An unpaired or paired two-tailed Student's *t*-test was used for *in silico* studies. Spearman's correlation coefficient was used to compare DNA copy number and mRNA expression levels. For *in vitro* studies, a two-tailed Student's *t*-test was performed to compare differences between the experimental groups. A multivariable Pearson chi-square test was used for clinical studies. All graphs were generated using GraphPad Prism version 8.4 (GraphPad Software, San Diego, CA, USA), and statistical analyses were performed using SPSS version 25 (SPSS, Chicago, IL, USA). In general, experiments were independently conducted in triplicate. Statistical significance was defined as $p<0.05$.

Declarations

Ethics approval and consent to participate

All procedures for clinical samples were performed after obtaining approval from the Institutional Review Board of the Seoul National University Dental Hospital (IRB number: ERI20021).

Consent for publication

All of the authors consent for publication.

Availability of data and materials

All publicly accessed data are available on databases described in methodology. Analyzed datasets used during the study can be made available from the corresponding author upon reasonable request.

Competing Interests

All authors declare that they have no conflict of interest.

Authors' contributions

M.-H.A. contributed to the conception, design, data acquisition, and analysis, and authored the original manuscript; J.-H.K., S.-J.C., H.-J.K., and D.-G.P. contributed to data acquisition and analyzed the *in silico* data; K.-Y.O., H.-J.Y., S.-D.H., and J.-I.L. participated in data analysis of the clinical samples; J.-A.S. and S.-D.C. contributed to the conception and design of experiments and supervised and authored the final manuscript. All authors approved the final manuscript and agreed to be responsible for all aspects of this work.

Acknowledgments

This work was supported by the National Research Foundation of Korea (NRF) grant funded by the Korea government (MSIT) (2019R1A2C1085896 and 2020R1C1C1005480).

References

1. Napolitano V, Tamagnone L. Neuropilins Controlling Cancer Therapy Responsiveness.Int J Mol Sci. 2019;20
2. Goel HL, Chang C, Pursell B, Leav I, Lyle S, Xi HS, Hsieh CC, Adisetiyo H, Roy-Burman P, Coleman IM, et al. VEGF/neuropilin-2 regulation of Bmi-1 and consequent repression of IGF-IR define a novel mechanism of aggressive prostate cancer. Cancer Discov. 2012;2:906–21.
3. Samuel S, Gaur P, Fan F, Xia L, Gray MJ, Dallas NA, Bose D, Rodriguez-Aguayo C, Lopez-Berestein G, Plowman G, et al. Neuropilin-2 mediated beta-catenin signaling and survival in human gastro-intestinal cancer cell lines. PLoS ONE. 2011;6:e23208.
4. Goel HL, Pursell B, Chang C, Shaw LM, Mao J, Simin K, Kumar P, Vander Kooi CW, Shultz LD, Greiner DL, et al. GLI1 regulates a novel neuropilin-2/alpha6beta1 integrin based autocrine pathway that contributes to breast cancer initiation. EMBO Mol Med. 2013;5:488–508.
5. Cao Y, Hoeppner LH, Bach S, Guo EG, Wang Y, Wu E, Cowley J, Chang MJ, Waddell DK. Neuropilin-2 promotes extravasation and metastasis by interacting with endothelial alpha5 integrin. Cancer Res. 2013;73:4579–90.
6. Roy S, Bag AK, Dutta S, Polavaram NS, Islam R, Schellenburg S, Banwait J, Guda C, Ran S, Hollingsworth MA, et al. Macrophage-Derived Neuropilin-2 Exhibits Novel Tumor-Promoting Functions. Cancer Res. 2018;78:5600–17.
7. Thomas NV, Kim SK. Beneficial effects of marine algal compounds in cosmeceuticals. Mar Drugs. 2013;11:146–64.
8. Tabarsa M, Karnjanapratum S, Cho M, Kim JK, You S. Molecular characteristics and biological activities of anionic macromolecules from Codium fragile. Int J Biol Macromol. 2013;59:1–12.
9. Kim J, Choi JH, Oh T, Ahn B, Unno T. Codium fragile Ameliorates High-Fat Diet-Induced Metabolism by Modulating the Gut Microbiota in Mice.Nutrients. 2020;12

10. Moon SM, Lee SA, Han SH, Park BR, Choi MS, Kim JS, Kim SG, Kim HJ, Chun HS, Kim DK, et al. Aqueous extract of Codium fragile alleviates osteoarthritis through the MAPK/NF-kappaB pathways in IL-1beta-induced rat primary chondrocytes and a rat osteoarthritis model. Biomed Pharmacother. 2018;97:264–70.
11. Jang B, Chung H, Jung H, Song HK, Park E, Choi HS, Jung K, Choe H, Yang S, Oh ES. Extracellular Vesicles from Korean Codium fragile and Sargassum fusiforme Negatively Regulate Melanin Synthesis. Mol Cells. 2021;44:736–45.
12. Dilshara MG, Jayasooriya RG, Kang CH, Choi YH, Kim GY. Methanol extract of Codium fragile inhibits tumor necrosis factor-alpha-induced matrix metalloproteinase-9 and invasiveness of MDA-MB-231 cells by suppressing nuclear factor-kappaB activation. Asian Pac J Trop Med. 2016;9:535–41.
13. Park HB, Hwang J, Zhang W, Go S, Kim J, Choi I, You S, Jin JO. Polysaccharide from Codium fragile Induces Anti-Cancer Immunity by Activating Natural Killer Cells.Mar Drugs. 2020;18
14. Park HB, Lim SM, Hwang J, Zhang W, You S, Jin JO. Cancer immunotherapy using a polysaccharide from Codium fragile in a murine model. Oncoimmunology. 2020;9:1772663.
15. Grandclement C, Borg C. Neuropilins: a new target for cancer therapy. Cancers (Basel). 2011;3:1899–928.
16. Wang J, Huang Y, Zhang J, Xing B, Xuan W, Wang H, Huang H, Yang J, Tang J. NRP-2 in tumor lymphangiogenesis and lymphatic metastasis. Cancer Lett. 2018;418:176–84.
17. Hong TM, Chen YL, Wu YY, Yuan A, Chao YC, Chung YC, Wu MH, Yang SC, Pan SH, Shih JY, et al. Targeting neuropilin 1 as an antitumor strategy in lung cancer. Clin Cancer Res. 2007;13:4759–68.
18. Jubb AM, Strickland LA, Liu SD, Mak J, Schmidt M, Koeppen H. Neuropilin-1 expression in cancer and development. J Pathol. 2012;226:50–60.
19. Chu W, Song X, Yang X, Ma L, Zhu J, He M, Wang Z, Wu Y. Neuropilin-1 promotes epithelial-to-mesenchymal transition by stimulating nuclear factor-kappa B and is associated with poor prognosis in human oral squamous cell carcinoma. PLoS ONE. 2014;9:e101931.
20. Rizzolio S, Cagnoni G, Battistini C, Bonelli S, Isella C, Van Ginderachter JA, Bernards R, Di Nicolantonio F, Giordano S, Tamagnone L. Neuropilin-1 upregulation elicits adaptive resistance to oncogene-targeted therapies. J Clin Invest. 2018;128:3976–90.
21. Chaudhary B, Khaled YS, Ammori BJ, Elkord E. Neuropilin 1: function and therapeutic potential in cancer. Cancer Immunol Immunother. 2014;63:81–99.
22. Houles T, Roux PP. Defining the role of the RSK isoforms in cancer. Semin Cancer Biol. 2018;48:53–61.
23. Sulzmaier FJ, Ramos JW. RSK isoforms in cancer cell invasion and metastasis. Cancer Res. 2013;73:6099–105.
24. Kang S, Elf S, Lythgoe K, Hitosugi T, Taunton J, Zhou W, Xiong L, Wang D, Muller S, Fan S, et al. p90 ribosomal S6 kinase 2 promotes invasion and metastasis of human head and neck squamous cell carcinoma cells. J Clin Invest. 2010;120:1165–77.

25. Davies AH, Reipas K, Hu K, Berns R, Firmino N, Stratford AL, Dunn SE. Inhibition of RSK with the novel small-molecule inhibitor LJI308 overcomes chemoresistance by eliminating cancer stem cells. Oncotarget. 2015;6:20570–7.
26. Li MY, Fan LN, Han DH, Yu Z, Ma J, Liu YX, Li PF, Zhao DH, Chai J, Jiang L, et al. Ribosomal S6 protein kinase 4 promotes radioresistance in esophageal squamous cell carcinoma. J Clin Invest. 2020;130:4301–19.
27. Fung TM, Ng KY, Tong M, Chen JN, Chai S, Chan KT, Law S, Lee NP, Choi MY, Li B, et al. Neuropilin-2 promotes tumourigenicity and metastasis in oesophageal squamous cell carcinoma through ERK-MAPK-ETV4-MMP-E-cadherin deregulation. J Pathol. 2016;239:309–19.
28. Cronin R, Brooke GN, Prischi F. The role of the p90 ribosomal S6 kinase family in prostate cancer progression and therapy resistance. Oncogene. 2021;40:3775–85.
29. Mishra VK, Johnsen SA. Targeted therapy of epigenomic regulatory mechanisms controlling the epithelial to mesenchymal transition during tumor progression. Cell Tissue Res. 2014;356:617–30.
30. Kalluri R, Weinberg RA. The basics of epithelial-mesenchymal transition. J Clin Invest. 2009;119:1420–8.
31. Dongre A, Weinberg RA. New insights into the mechanisms of epithelial-mesenchymal transition and implications for cancer. Nat Rev Mol Cell Biol. 2019;20:69–84.
32. Lamouille S, Xu J, Derynck R. Molecular mechanisms of epithelial-mesenchymal transition. Nat Rev Mol Cell Biol. 2014;15:178–96.
33. Sanchez-Tillo E, Lazaro A, Torrent R, Cuatrecasas M, Vaquero EC, Castells A, Engel P, Postigo A. ZEB1 represses E-cadherin and induces an EMT by recruiting the SWI/SNF chromatin-remodeling protein BRG1. Oncogene. 2010;29:3490–500.
34. Nilsson GM, Akhtar N, Kannius-Janson M, Baeckstrom D. Loss of E-cadherin expression is not a prerequisite for c-erbB2-induced epithelial-mesenchymal transition. Int J Oncol. 2014;45:82–94.
35. Saitoh M. Involvement of partial EMT in cancer progression. J Biochem. 2018;164:257–64.
36. Luond F, Sugiyama N, Bill R, Bornes L, Hager C, Tang F, Santacroce N, Beisel C, Ivanek R, Burglin T, et al. Distinct contributions of partial and full EMT to breast cancer malignancy. Dev Cell. 2021;56:3203–21. e3211.
37. Trepat X, Chen Z, Jacobson K. Cell migration. Compr Physiol. 2012;2:2369–92.
38. Sibley LD, Dobrowolski J, Morisaki JH, Heuser JE. Invasion and Intracellular Survival by Toxoplasma-Gondii. Bailliere Clin Inf D. 1994;1:245–64.
39. Novikov NM, Zolotaryova SY, Gautreau AM, Denisov EV. Mutational drivers of cancer cell migration and invasion. Br J Cancer. 2021;124:102–14.
40. Hua X, Huang M, Deng X, Xu J, Luo Y, Xie Q, Xu J, Tian Z, Li J, Zhu J, et al. The inhibitory effect of compound ChlA-F on human bladder cancer cell invasion can be attributed to its blockage of SOX2 protein. Cell Death Differ. 2020;27:632–45.

Figures

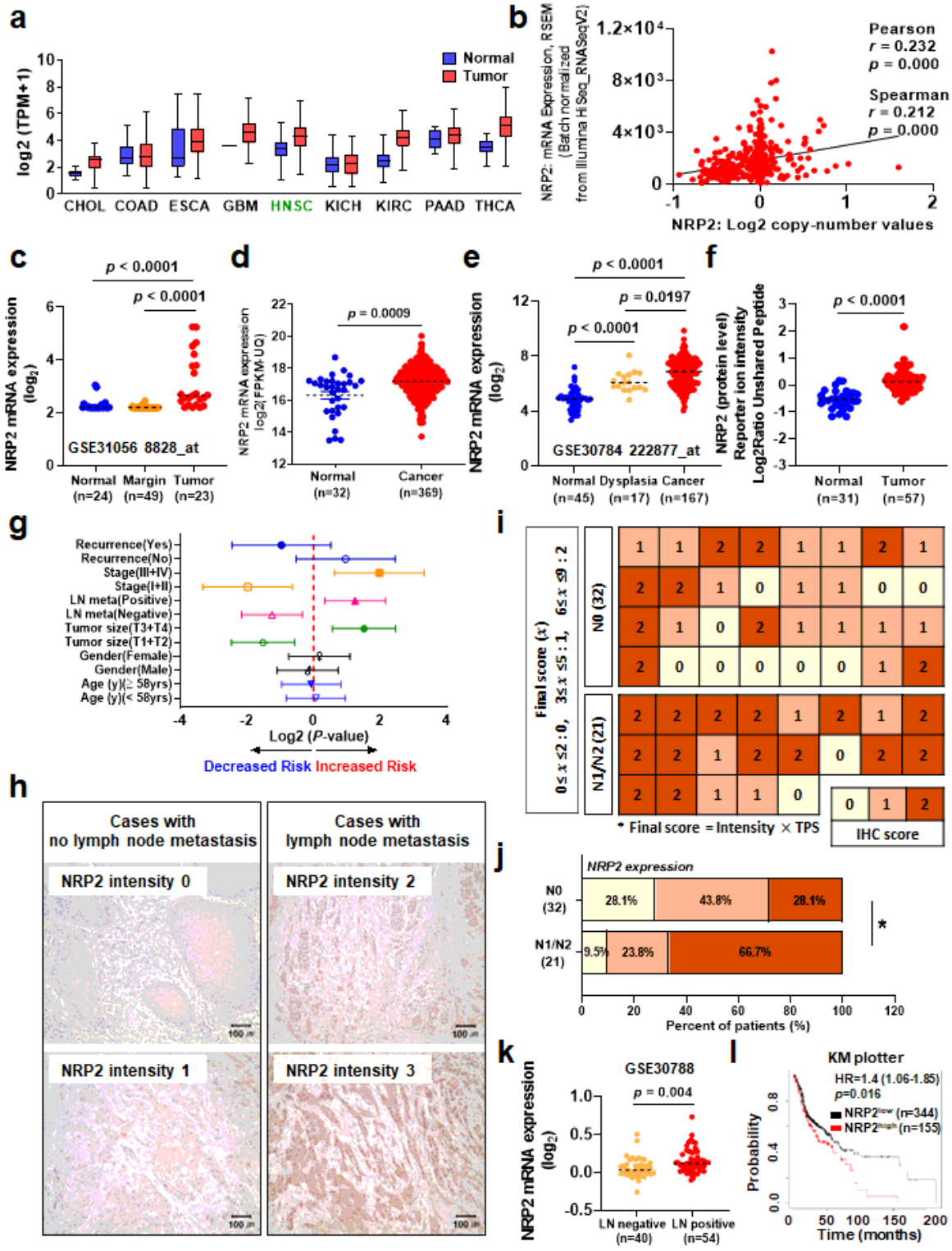

Figure 1

NRP2 is aberrantly expressed and associated with worse prognosis in human HNC. **a** The expression levels of NRP2 between normal tissues and 9 kinds of human cancer tissues were evaluated using the ULACAN. **b** Correlation analysis between *NRP2* copy number and the corresponding mRNA levels in 488

HNC samples was investigated using cBioPortal. The correlation coefficients were evaluated by Pearson's and Spearman's correlation tests. **c** Comparison of NRP2 mRNA expression levels between normal, margin, and OSCC tissues from the GEO dataset (GSE31056 8828_at). **d** NRP2 mRNA expression between normal oral epithelium and HNC tissues from the TCGA dataset. **e** NRP2 mRNA expression between normal oral epithelium, dysplasia, and OSCC tissues from the GEO dataset (GSE30784 222877_at). **f** Comparison of NRP2 protein levels between normal oral epithelium and HNC tissues from the CPTAC. **g** Forest plot showing relative risks (RR) of OSCC patients with NRP2 expression. **h** Representative IHC images representing the association between NRP2 intensity and LNM in 53 patients with OSCC. Scale bar: 100 μm. **i** Graphical images of the NRP2 expression pattern showing the relationship between the IHC score of NRP2 and the degree of the spread to regional LNs in 53 OSCC tissues. **j** Stacked bar graph demonstrating the percentage of the NRP2 expression according to the N classification. **k** Comparison of the NRP2 mRNA expression levels between LN-negative and LN-positive HNC samples from GEO dataset (GSE30788). **l** KM plotter analysis indicating the association between NRP2 expression levels and survival rate in HNC patients.

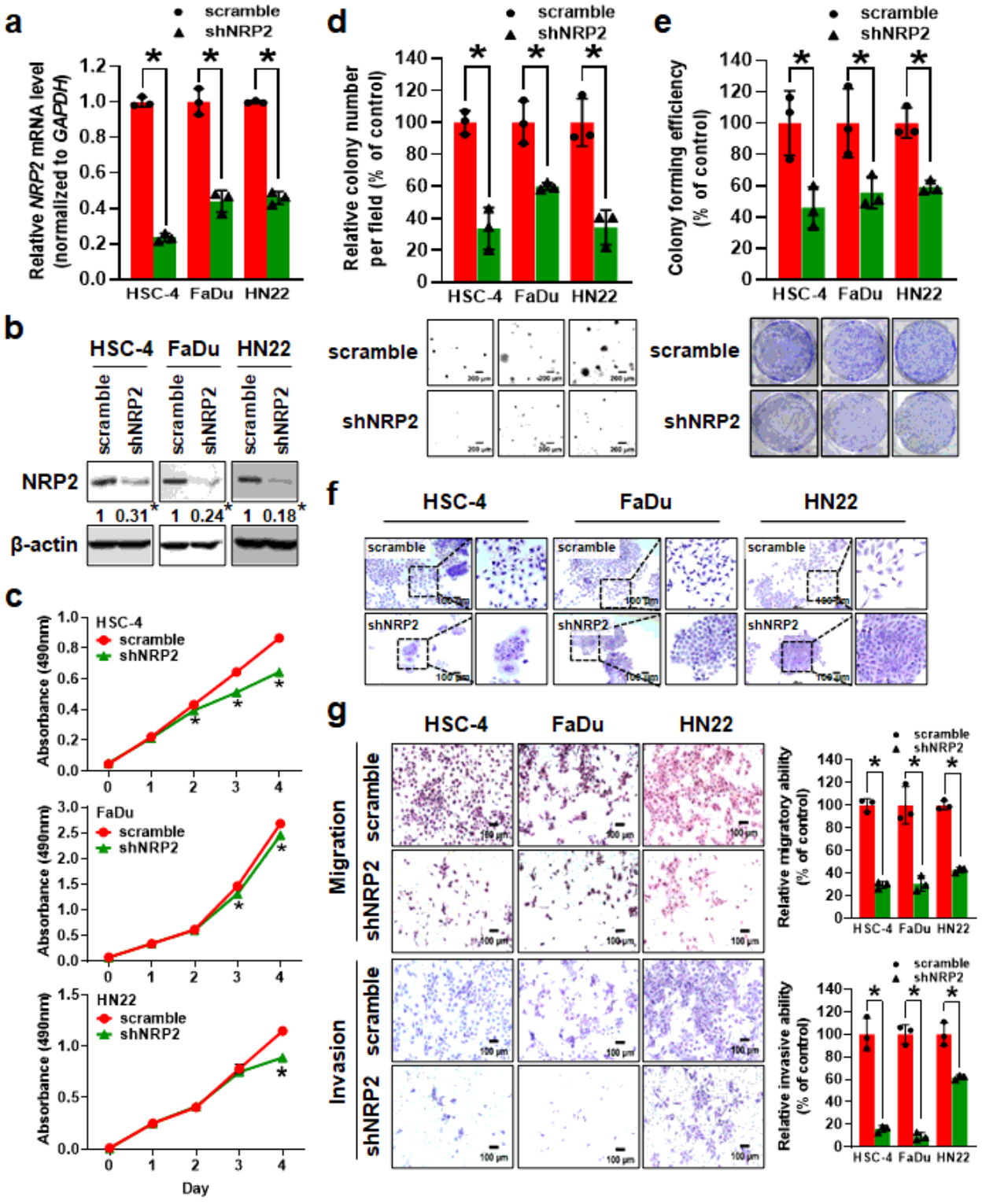

Figure 2

NRP2 promotes cell proliferation, motility, and invasiveness in human HNC cells. **a** The qPCR result showing the *NRP2* mRNA levels in NRP2-silencing HNC cells. The *GAPDH*was used as the reference gene for normalization. **b** Immunoblotting images showing the NRP2 protein levels in NRP2-silencing HNC cells. The β-actin was used as the loading control. **c** The proliferation of NRP2-silencing HNC cells was determined by MTS assay. **d** The anchorage-independent growth of NRP2-silencing HNC cells was

analyzed by the soft agar assay (top panel). Representative images from the soft agar assay (bottom panel). Scale bar: 200 μm. **e**The colony-forming efficiency of NRP2-silencing HNC cells was assessed by clonogenic assay (top panel). Representative images from the clonogenic assay (bottom panel). **f** Representative morphologic images of NRP2-silencing HNC cells. The images from the clonogenic assay were visualized after crystal violet staining. Scale bar: 100 μm. **g** Representative images showing the migratory or invasive ability of NRP2-silencing HNC cells (left panel). Scale bar: 100 μm. Bar graph represents the results from transwell migration or invasion assays (right panel). All results are expressed as the mean ± standard deviation (SD) of three independent experiments. *p< 0.05 by two-tailed Student's t-test.

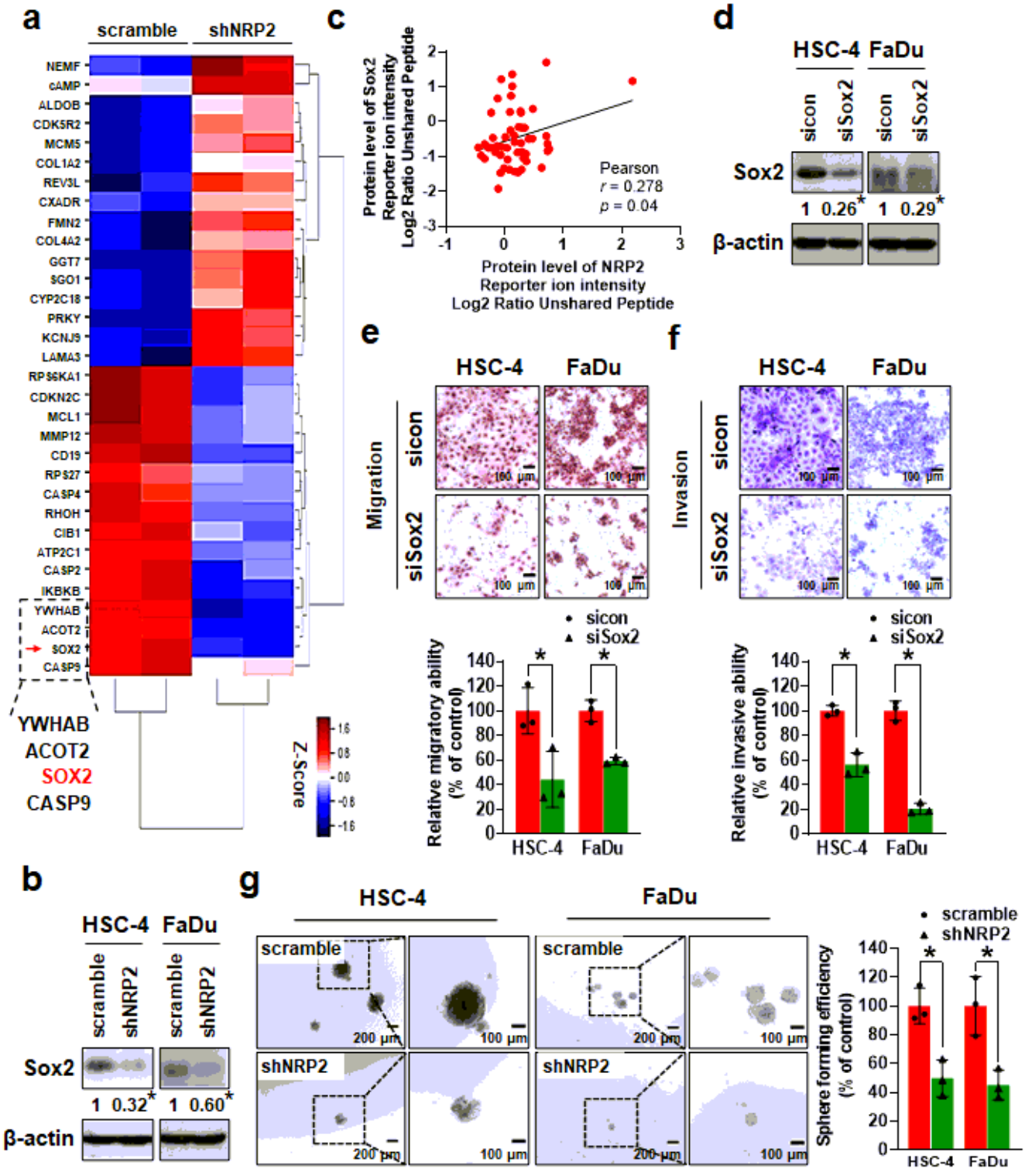

Figure 3

NRP2 enhances the aggressiveness and CSC properties of human HNC cells by regulating Sox2. **a**Hierarchical clustering analysis depicting 32 proteins with a fold shift greater than 1.2 in NRP2-silencing HSC-4 cell line compared with the control group. Z-score is represented as red (high expression) and blue (low expression). **b** Immunoblotting image showing the Sox2 expression levels in NRP2-silencing HNC cells. The β-actin was used as the loading control. **c** Correlation analysis between NRP2 and Sox2 protein

levels in HNC samples using CPTAC. The correlation coefficient was evaluated by Pearson's correlation test. **d** Immunoblotting images showing the Sox2 expression levels in siRNA-transfected cells. The β-actin was used as the loading control. **e–f** Representative images demonstrating the migratory (e) or invasive ability (f) of siRNA-transfected cells (top panel). Scale bar: 100 μm. Bar graph represents the results from transwell migration or invasion assays (bottom panel). **g** Representative images of spheres formed in NRP2-silencing HNC cells (left panel) compared with the control group. Scale bar: 100 or 200 μm. Bar graph indicates sphere-forming efficiency (right panel). All results are expressed as the mean ± SD of three independent experiments. *$p < 0.05$ by two-tailed Student's t-test.

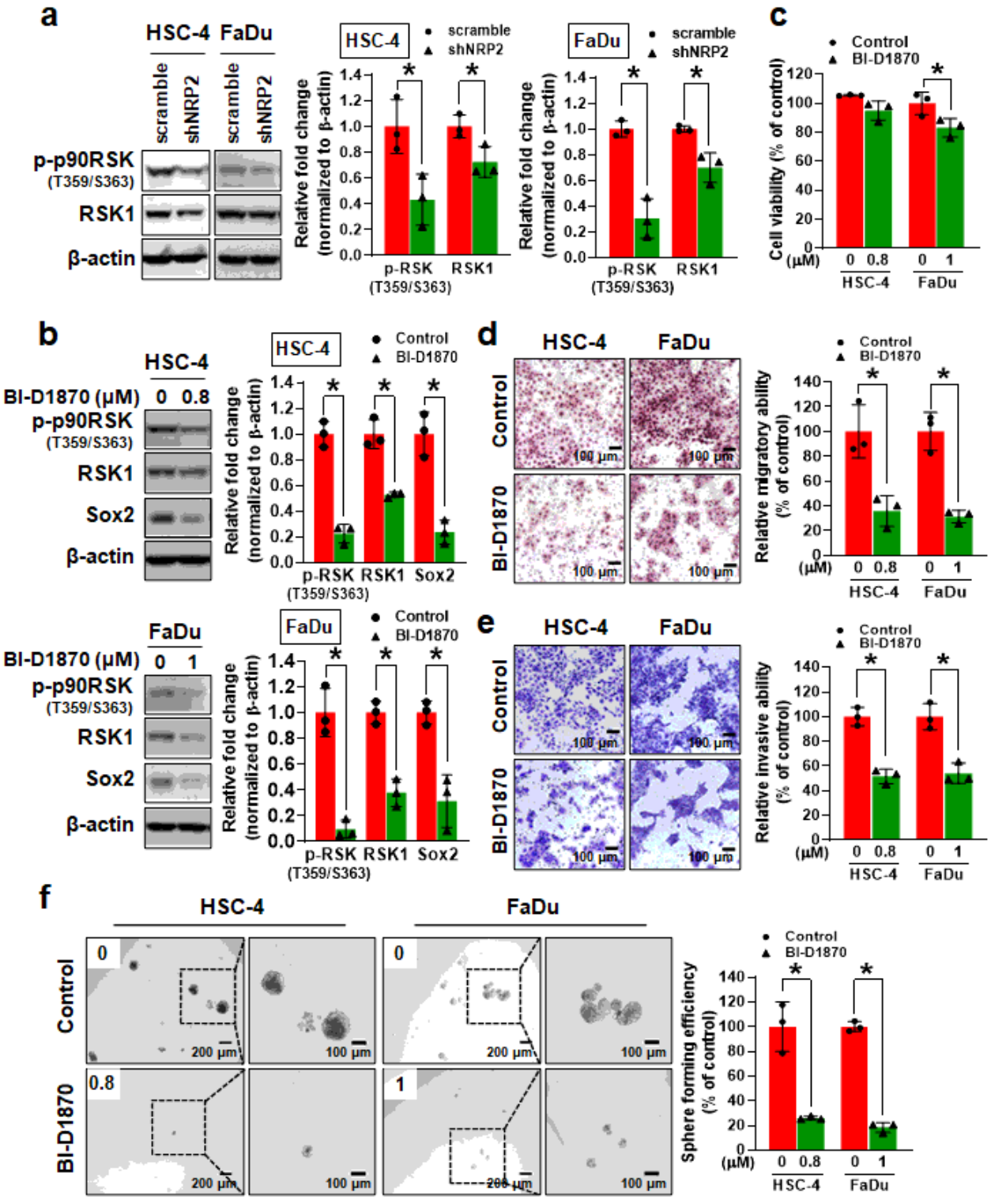

Figure 4

RSK1 mediates between NRP2 and Sox2 to encourage aggressive behaviors of human HNC cells. **a** Immunoblotting images showing the expression levels of p-p90RSK and RSK1 in NRP2-silencing HNC cells. The β-actin was used as the internal control. **b** Cells were treated with indicated concentrations of BI-D1870 (24 h for HSC-4 and 48 h for FaDu). Protein levels of p-p90RSK, RSK1, and Sox2 in HNC cells treated with BI-D1870. The β-actin was used as the internal control. **c** The cell viability was evaluated by

trypan blue exclusion assay. **d-e** Representative images showing the migratory (d) or invasive ability (e) of HNC cells treated with BI-D1870 (left panel). Scale bar: 100 μm. Bar graphs represent the results from transwell migration or invasion assays (right panel). **f** Representative images of spheres formed in BI-D1870-treated cells (left panel) compared with the control group. Scale bar: 100 or 200 μm. Bar graph indicates sphere-forming efficiency (right panel). All results are expressed as the mean ± SD of three independent experiments. *$p < 0.05$ by two-tailed Student's t-test.

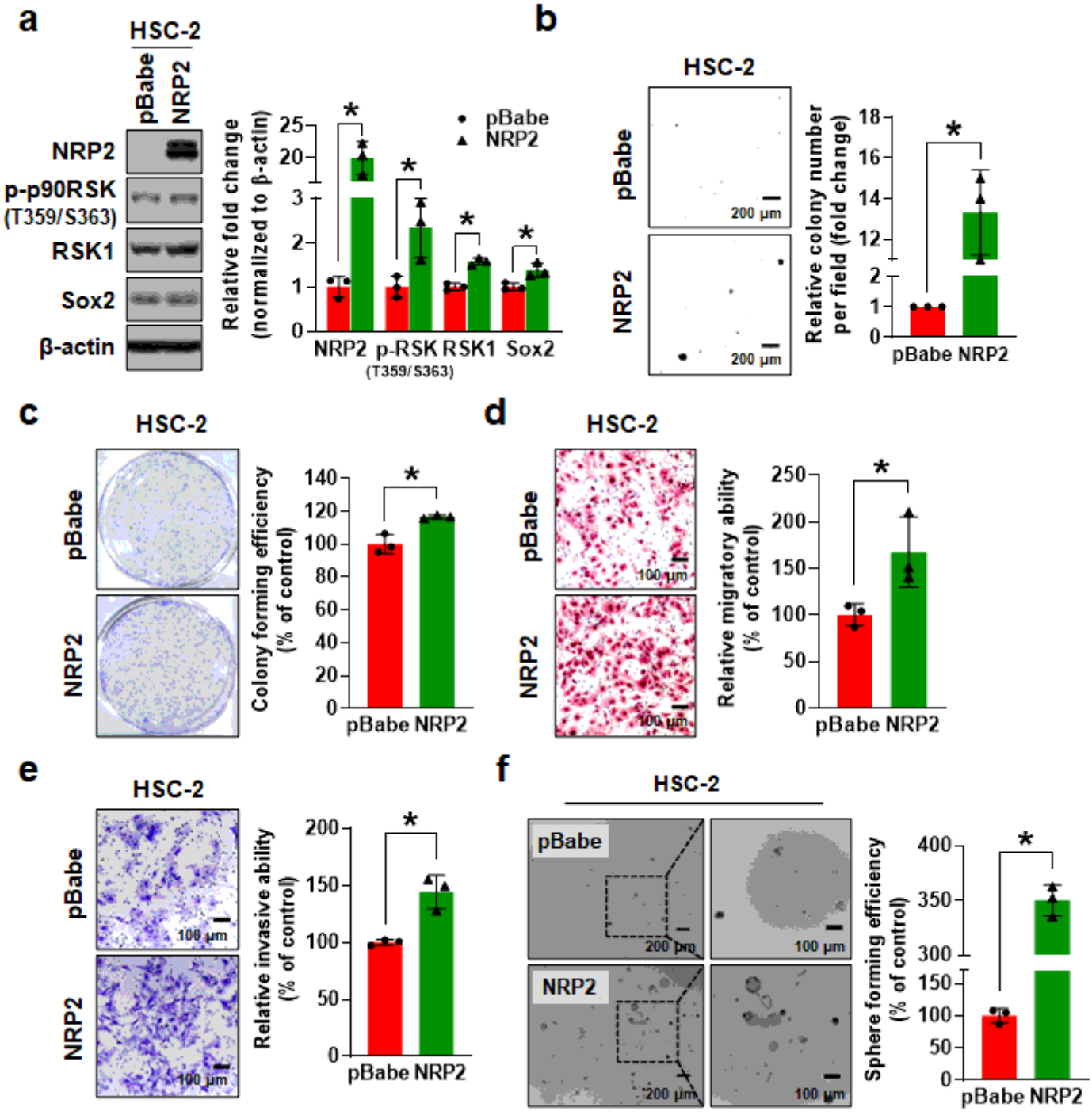

Figure 5

NRP2 orchestrates proliferation and aggressive behaviors of human HNC cells by facilitating the RSK1/Sox2 axis. **a** Protein levels of NRP2, p-p90RSK, RSK1, and Sox2 in NRP2-overexpresssing cells. The β-actin was used as the internal control. **b** Representative images from the soft agar assay in NRP2-overexpressing cells. Scale bar: 200 μm. **c** Representative images from the clonogenic assay in NRP2-overexpressing cells. **d-e** Representative images showing the migratory (d) or invasive ability (e) of NRP2-overexpressing cells (left panel). Scale bar: 100 μm. Bar graphs represent the results from transwell migration or invasion assays (right panel). **f** Representative images of spheres formed in NRP2-overexpressing cells compared with the control group. Scale bar: 100 or 200 μm. All results are expressed as the mean ± SD of three independent experiments. *$p < 0.05$ by two-tailed Student's t-test.

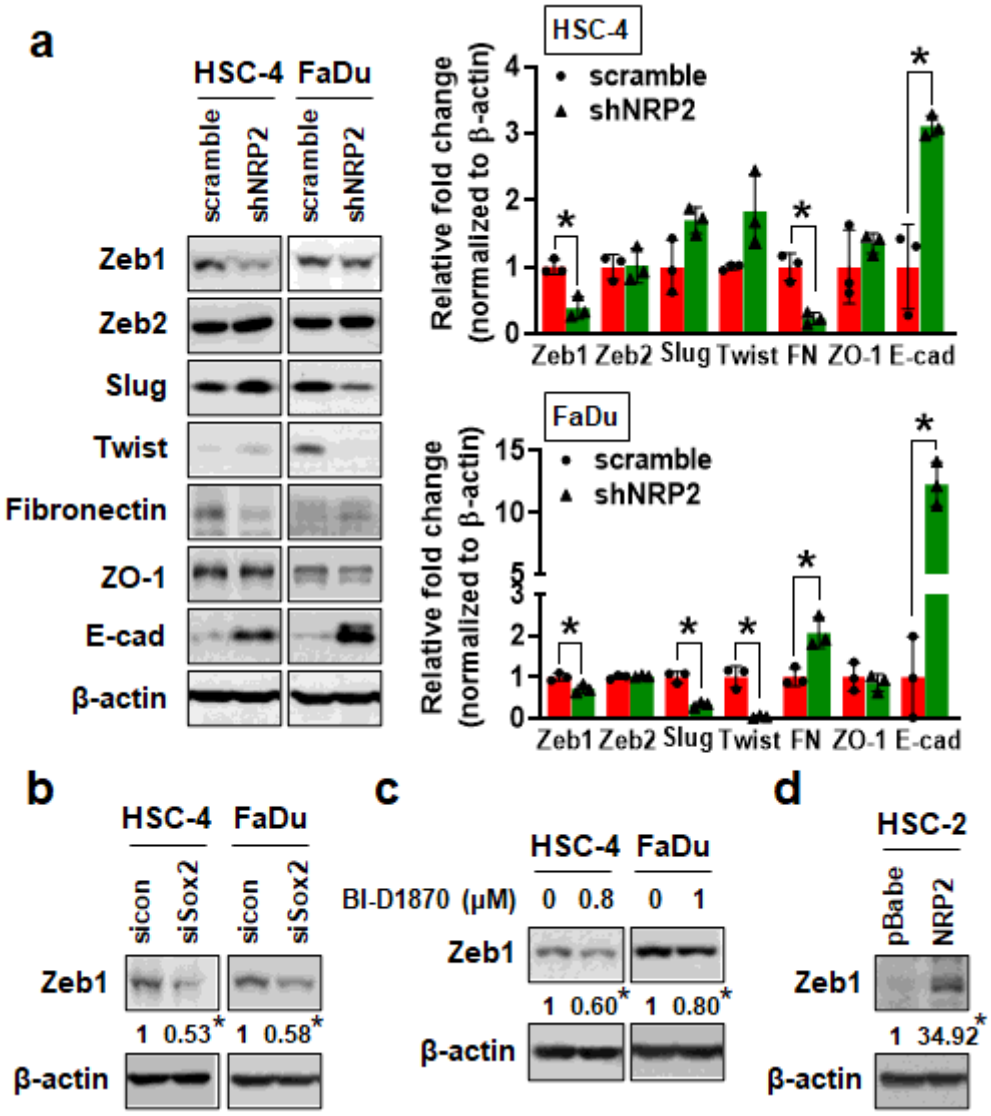

Figure 6

Zeb1 is necessary for the EMT progression of human HNC cells during the NRP2/RSK1/Sox2 signaling pathway. **a** Immunoblotting images showing the expression levels of EMT markers in NRP2-silencing HNC cells. **b-d**Immunoblotting images from siRNA-transfected (b), BI-D1870-treated (c), or NRP2-

overexpressing cells (d). The β-actin was used as the internal control. All results are expressed as the mean ± SD of three independent experiments. *$p < 0.05$ by two-tailed Student's t-test.

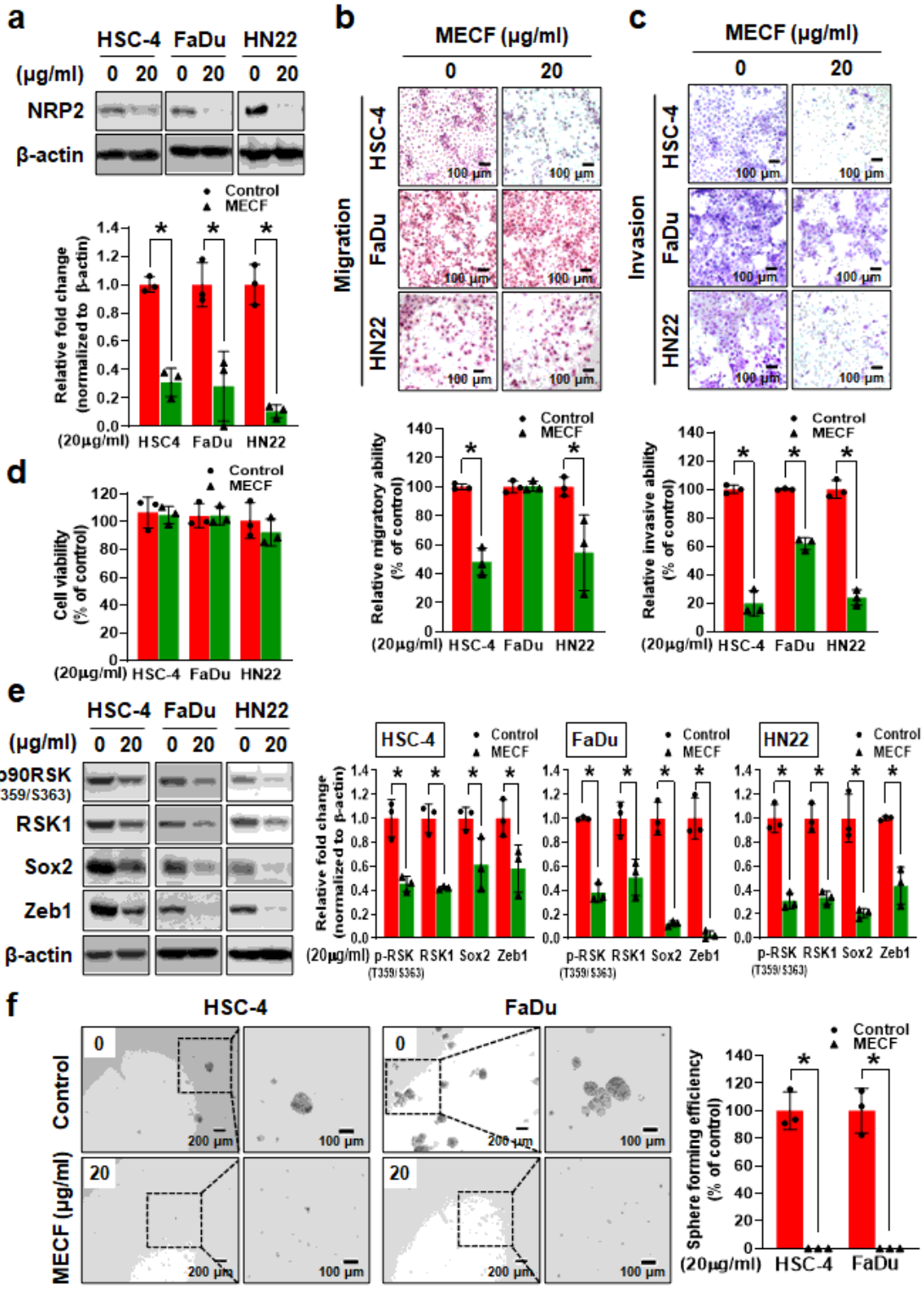

Figure 7

MECF suppresses the aggressive behaviors of human HNC cells through inhibition of the NRP2/RSK1/Sox2/Zeb1 signaling pathway. **a** Immunoblotting image of the expression levels of NRP2 in

MECF-treated cells. The β-actin was used as the loading control. **b-c** Representative images showing the migratory (b) or invasive ability (c) of MECF-treated cells compared with the control group (top panel). Scale bar: 100 μm. Bar graphs represent the results from transwell migration or invasion assays (bottom panel). **d** Cell viability was evaluated by a trypan blue exclusion assay. **e** Immunoblotting images of the expression levels of p-p90RSK, RSK1, Sox2, and Zeb1 in MECF-treated cells. The β-actin was used as the loading control. **f** Representative images of spheres formed in MECF-treated cells compared with the control group. Scale bar: 100 or 200 μm. All results are expressed as the mean ± SD of three independent experiments. *$p < 0.05$ by two-tailed Student's t-test.

Supplementary Files

This is a list of supplementary files associated with this preprint. Click to download.

- Additionalfile1SupplementaryInformations.docx
- graphicalabstract.tif